Real driving particle number (PN) emissions from China-6 compliant PFI and GDI hybrid electrical vehicles

Zhengjun Yang[1], Yunshan Ge[1], Daisy Thomas[2], Xin Wang[1]*, Sheng Su[1], Hu Li[2], Hongwen He[1]

1. School of Mechanical Engineering, Beijing Institute of Technology, Beijing 100081, China

2. School of Chemical and Process Engineering, University of Leeds, Leeds LS2 9JT, UK

Corresponding author: Xin Wang Ph.D

Address: National Laboratory of Automotive Performance & Emission Test, School of Mechanical Engineering, Beijing Institute of Technology, Beijing 100081, China

Tel./Fax: +86 10 68912035

E-mail: xin.wang@bit.edu.cn

Abstract:

In this paper, the real driving particle number (PN) emissions from two China-6 compliant hybrid electrical vehicles (HEVs) were measured using a certification-level portable emission measurement system (PEMS) and strict adherence to the regulatory procedures for real driving emission (RDE) testing. The results show that the trip-averaged PN emission factors for the port fuel injection (PFI) HEV and the gasoline direct injection (GDI) HEV were 1.15E+12 and 1.71E+12#/km respectively, much higher than the engine-only counterparts and failing the existing RDE limits. Enriched air-fuel mixtures and probably lowered catalyst conversion efficiencies as a result of more frequent engine stop-and-goes of the HEVs are found to be the underlying reasons for the extra PN emissions. The test results also suggest the necessity to amend the power management strategy currently widely used in HEVs to deal with the PN issue.

Key words: particle number; real driving emission; hybrid vehicles; port fuel injection; gasoline direct injection

1. Introduction

Globally, ground vehicle electrification is becoming ever more popular, due to several unprecedented CO_2 abatement goals set for the transport sector. In regard to the comparably short range and high cost of battery electric vehicles (BEVs), partially electrified vehicles, namely hybrid electric vehicles (HEVs) and plug-in HEVs, seem more feasible and practical in the short-term. Undoubtedly, HEVs exhibit remarkable fuel economies and therefore CO_2 reduction advantages over ICE-only vehicles, particularly in combination with plug-in technology and bio-fuels (Graver et al. 2011)(Sioshansi and Denholm 2009). A previous study reported a greater than 80% decrease in life-cycle greenhouse gas emissions from a bio-methane fueled, engine optimized 2nd Gen Toyota Prius (Bordelanne et al. 2011). Several laboratory and real-world emission tests as well as case studies also demonstrated lower regulated emissions from HEVs compared to ICE-only counterparts (Sioshansi and Denholm 2009)(Wu et al. 2015)(Al-Samari 2017)(O'Driscoll et al. 2018). However, little attention has been paid to the particle number (PN) emissions from HEVs so far, to some degrees, due to the absence of certification and in-service compliance requirements.

Currently, PN is mandatory during the certification of new diesel and gasoline direct injection (GDI) vehicles in the EU. Whilst in China, along with the promulgation of light-duty China-6, a fuel-neutral and technology-neutral regulation has been effective in Shenzhen since Nov, 2018, all new vehicles, even port fuel injection (PFI) gasoline and natural gas (NG) vehicles, must comply with the not-to-exceed (NTE) PN limit of 6E+11 particles per kilometer traveled (#/km) for a laboratory test over the WLTC and the NTE limit of 1.26E+12#/km for RDE.

Although the measurement of PN could have higher variations than PM, PN is of equal importance to particulate mass (PM) given its significance as a complementary metric to regulate ultrafine particles and their related adverse environmental and health impacts (David B Kittelson 1998)(Hesterberg et al. 2012).

A number of studies have been conducted to disclose the PN emissions and their size-resolved distributions of engines and vehicles since 2010 (Yin et al., 2013) (Liu et al., 2017). The most recent ones are reported by Wang (2018) and Mendoza-Villafuerte et al. (2017), but these studies were primarily performed on non-hybrid vehicles. In terms of the PN emissions from HEVs, the majority of existing research focused on heavy-duty vehicles. (Soylu, 2015)(Wang, 2017)(Kean et al. 2000)(Xu, 2017).

Regarding light-duty vehicles, Robinson and Holmén (2011) compared the PN emissions from a conventional Toyota Camry and a hybrid one using a TSI EEPS spectrometer. Much higher real-world PN emissions were found with the hybrid test vehicle, which was attributed to the extremely high PN emissions at each engine restart. This conclusion accorded well with Christenson et al.(2007), who used an ELPI for the testing of four market-available hybrid cars under various real-driving conditions and concluded orders of magnitude higher PN emissions from the hybrid vehicles relative to the conventional car. A limitation of the prior studies is the use of non-regulatory method for the on-board measurement of PN, primarily due to the unavailability of such equipment at that time, which may increase the difficulty of cross-reference evaluation since as summarized by Kittelson et al. (2006), the results yielded from these impactors could be to various degree lower than a regulatory condensed particle counter (CPC).

In view of the current scarcity of real driving PN studies for light-duty hybrid vehicles, especially GDI-powered ones, and to check whether the previously reported PN issue with hybrid vehicles still exists on modern models, this paper tested two hybrid vehicles (PFI- and GDI-powered each) according to the legislative RDE procedures, to investigate how hybrid technologies impact the real driving PN emissions from in-use cars and call attention to hybrid PN issue.

2. Test equipment and procedure

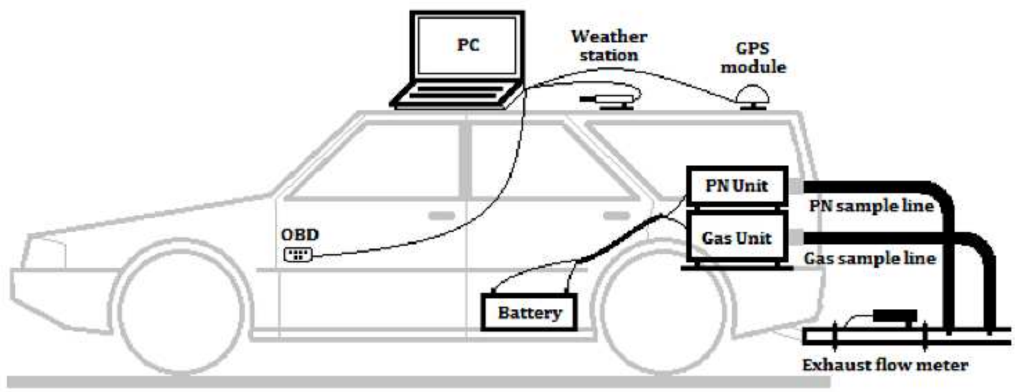

Fig.1 PEMS configuration for real driving emissions testing

As shown in Fig.1, the real-world PN emissions of the two test vehicles were measured using a state-of-the-art PEMS (HORIBA OBS-ONE, Japan) and according to the EU Real Driving Emission (RDE) test protocol Package 1-3. The PEMS mainly consists of a gas module, a PN module, and a pitot exhaust flow meter. The gas module can measure CO, CO_2, and NO_x while the PN module measures total PN using a PMP-compliant CPC with a thermal denuder mounted prior to its sample inlet. As regulated, only the particles with aerodynamic diameters larger than 23nm will be counted by the system. When testing, the thermal denuder was heated to 300°C to remove any light-molecular-weight volatile material or water vapor that may result in measurement artifacts via condensation mechanisms. The PN sampling probe was placed next to the exit of the exhaust flow meter, where a thermocouple for exhaust temperature was also fitted, but prior to the sampling probe of the gaseous pollutants to minimize the influence of turbulence on PN measurement.

Two 12V batteries were employed to power the testing system. Real-time information including the concentrations of PN and gaseous pollutants, location, altitude, ambient temperature, and humidity, were outputted per second and saved to a laptop via wire connections. The laptop also acquired some real-time engine operating parameters of the test vehicles from the OBD over the entire test trip. Time-alignment of the OBD data, exhaust flow rates and pollutant concentrations were automatically accomplished by a self-programmed program for data post-processing. The trip-averaged PN emissions of the two test vehicles were calculated using the Moving Average Window method, also called EMROAD elsewhere. The stepwise description of EMROAD calculation can be found in the document of Euro-6. It should be also clarified that the tailpipe emissions measured within the engine-start, warm-up and idle were all included in the calculation of trip-averaged emission factors, in line with the draft of the 4th RDE Package.

Table.1 Specifications of the test vehicles

Car No.	Engine type	Model year	After-treatment	Mileage	Emission category
1	In-line, 4 cyl, Atkinson-cycle, 1.8L NA PFI, 73kW	2017/18	Stoichiometric TWC	6065	China-6
2	In-line, 4 cyl, Atkinson-cycle, 2.0L NA GDI, 115kW,	2017/18	Stoichiometric TWC	13722	China-6

Table.1 lists the key specifications of the two hybrid vehicles tested in this paper. Both models are among the best-selling hybrid vehicles in China so considered to have good representativeness. Both test vehicles were China-6 certified and well-maintained. Before the RDE testing, both vehicles were tested in a certification laboratory based in Beijing to ensure their status was suitable for RDE test and acquire the CO_2 emissions for the use as the reference of trip normality verification.

Both vehicles were fed with RON92, China-6 compliant gasoline purchased from a certified supplier. The requirement of China-6 gasoline standard includes but is not confined to sulfur≤10ppm, benzene≤0.8vol%, aromatics≤35vol%, olefins≤18vol% and prohibits the use of Mn- or Fe-containing additives.

As mandated, the RDE test route used in this paper comprised urban, rural and highway driving stages. In the RDE regulation, urban driving is defined as driving under 60km/h. Driving faster than 60km/h but not exceeding 90km/h belongs to rural driving, while driving above 90km/h is categorized as highway driving. The distance-based portions of urban, rural and highway driving in a valid RDE trip shall be 34%, 33%, and 33% respectively with a ±10% allowance (urban must be above 29%). To ensure the driving style of the tests was fair enough so as to represent cars' normal operations, two metrics, namely $v.a_{pos}$-[95] and RPA, were introduced for evaluation purpose. Both test vehicles passed the verifications. The definitions of $v.a_{pos}$-[95] and RPA, and more detailed requirements of the Euro-6 RDE testing can be found on the official website of the European Commission.

Table.2 Summary of the test conditions and PN emissions from the tested HEVs in real-world driving

		Urban						Rural+highway					
Test car	Trip-averaged PN (#/km)	Trip distance (km)	Ave. speed (km/h)	Time (s)	No. of engine-start (1)	PN emission factor (#/km)	PN share (%)	Trip distance (km)	Ave. speed (km/h)	Time (s)	No. of engine-start (1)	PN emission factor (#/km)	PN share (%)
PFI	1.15E+12	21.82	24.4	3220	107	3.3E+12	82	54.59	78.29	2510	48	2.94E+11	18
GDI	1.71E+12	20.4	23.17	3170	23	1.91E+12	33	48.76	76.18	2305	39	1.63E+12	67

The PEMS was calibrated with pure nitrogen and CO, CO_2, NO-blended span gas of known concentrations before and after the RDE trips to guarantee that zero-drift and pollutant readings were always within the regulated ranges. For each vehicle, RDE tests were performed strictly in accordance with the regulatory procedures and repeated until all the boundary conditions, including the normality, completeness and dynamic parameters, were met. The "standard" drive mode of the test vehicles was used in testing, as mandated by the regulation. Typically, an RDE trip lasted for

90 to 120 minutes and ran 60 to 80km, more details and the test results are summarized in Table.2. All the tests were performed in September, 2017 in Beijing, where the altitude is about 70m and the ambient temperature and relative humidity were 23-28°C and 25-35% respectively.

3. Result and discussion

3.1 Comparably higher RDE PN from HEVs

Fig.2 compares the real driving PN emissions from the two HEVs and their ICE-only counterparts. Both counterparts were from the same manufacturers as the HEVs tested in this paper. To secure persuadable comparability in between, the engine displacements and technical levels, vehicle sizes and curb weights were kept as similar as possible when selecting the counterparts.

It can be seen in Fig.2 that the real driving PN emissions from the HEVs are far higher than those from the ICE-only counterparts, especially for the PFI group, the gap has been up to an order of magnitude. A comparison with the EU and China limit values also demonstrates that only the HEVs fail the future RDE-PN requirements. In order to investigate the reasons underlying such high real driving PN emissions from the HEVs, the second-by-second PN emissions of the two tested HEVs are analyzed against a series of OBD available parameters and discussed below.

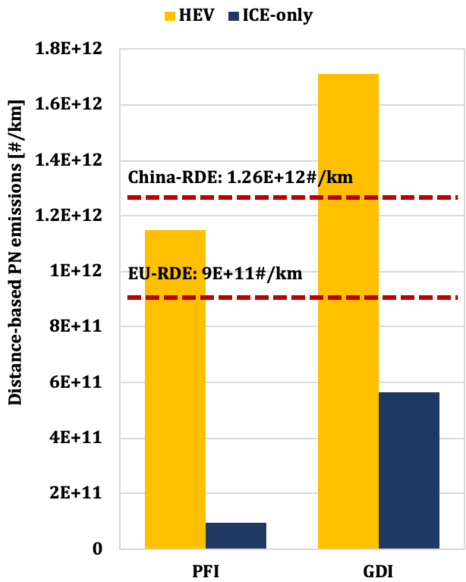

Fig.2 Real driving PN emissions from hybrid vehicles and their gasoline counterparts

3.2 PN emissions in urban driving

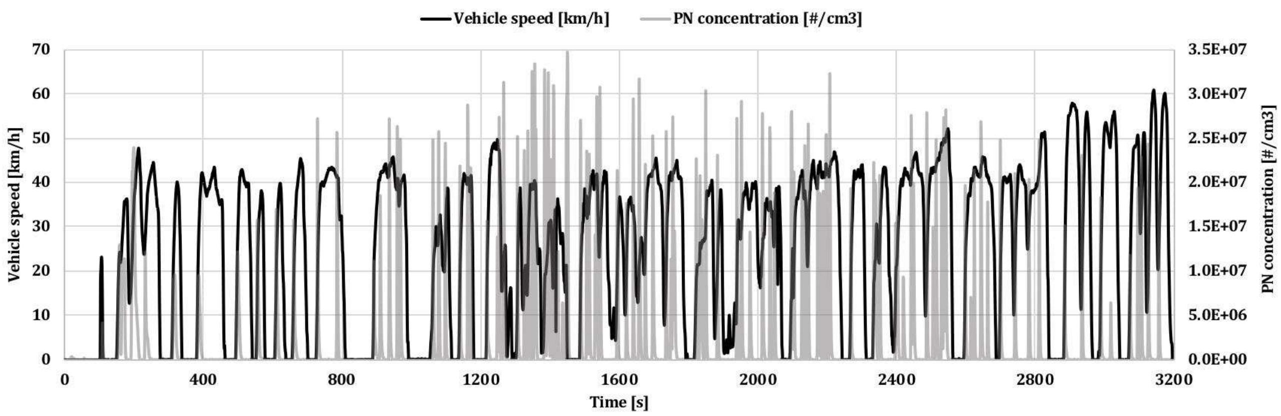

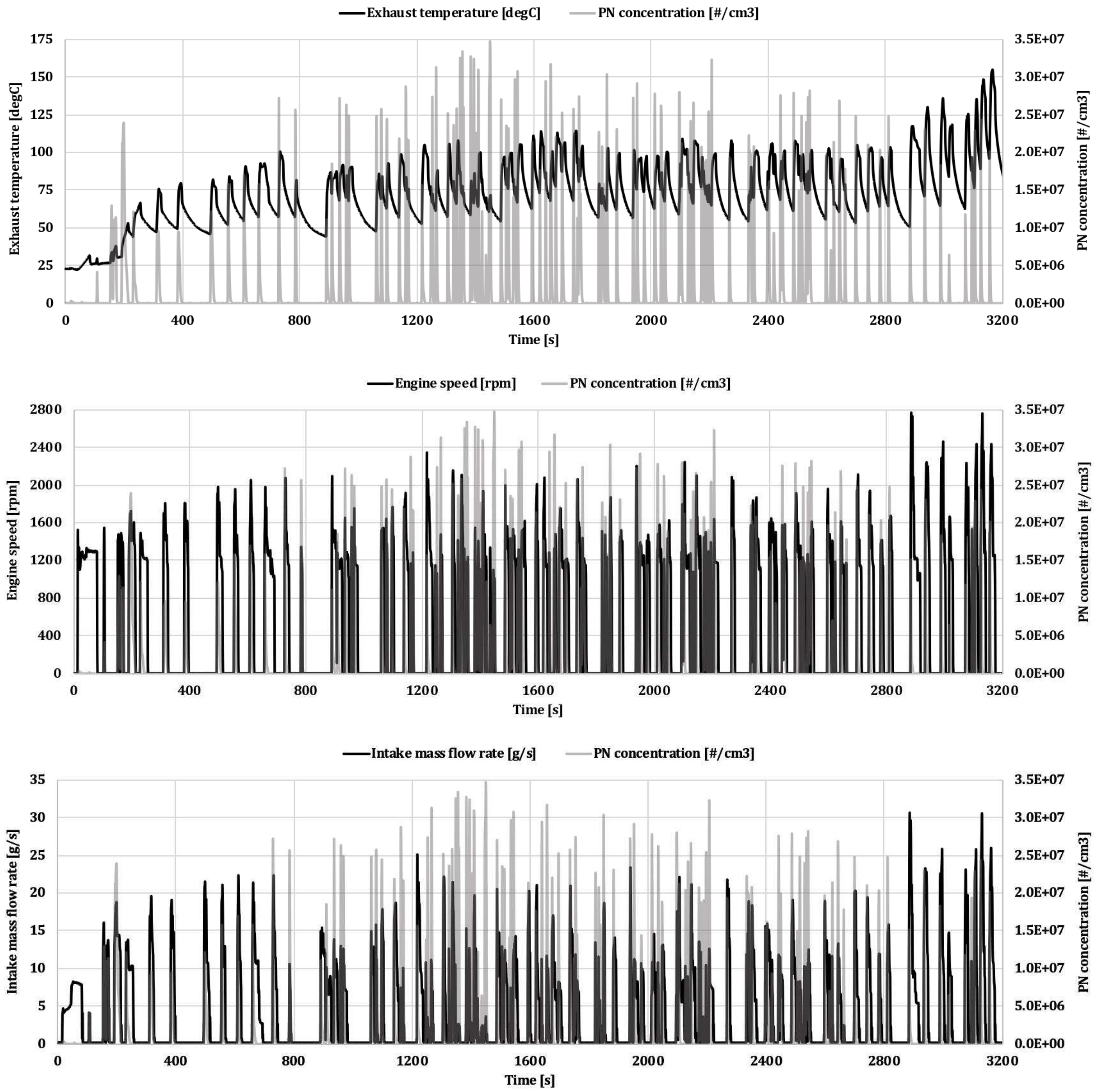

Fig.3 Vehicle speed, engine speed, exhaust temperature, and intake mass flow rate vs. PN concentration of the PFI-HEV within the urban driving stage

In Fig.3, the modal data of vehicle speeds, engine speeds, exhaust temperatures, and intake mass flow rates of the PFI-hybrid test vehicle are plotted versus PN concentrations. Plenty of PN spikes can be seen in the figure throughout the urban driving period. Many of these PN spikes linking to engine-starts show very high amplitudes, some of them being even higher than 3.0E+7 particles per cubic centimeter (#/cm^3), which is roughly 1000 times dirtier than the concentrations seen when the engine was on.

The high-PN events in Fig.3 are perfectly consistent with engine-starts (see engine speed and intake mass flow rate vs. PN), inferring that the formation of extra PN emissions may be a consequence of transient operating of the engine, which agrees with Robinson and Holmén (2011). Fig.4 supports this hypothesis by illustrating the second-by-second CO emissions in context to PN. It can be clearly seen in Fig.4 that almost every PN spike corresponds to a CO peak, no matter the CO concentration was high or comparably low. In theory, extra CO generated during the normal operation of an engine is an indicator of enriched combustion in-cylinder, and the overall insufficiency of oxygen in-cylinder can result in an increase in the particulate emissions. Hence, it is reasonable to conclude that enriched combustion occurred within frequent engine-start events was a reason for the extreme PN emissions from this PFI-hybrid vehicle.

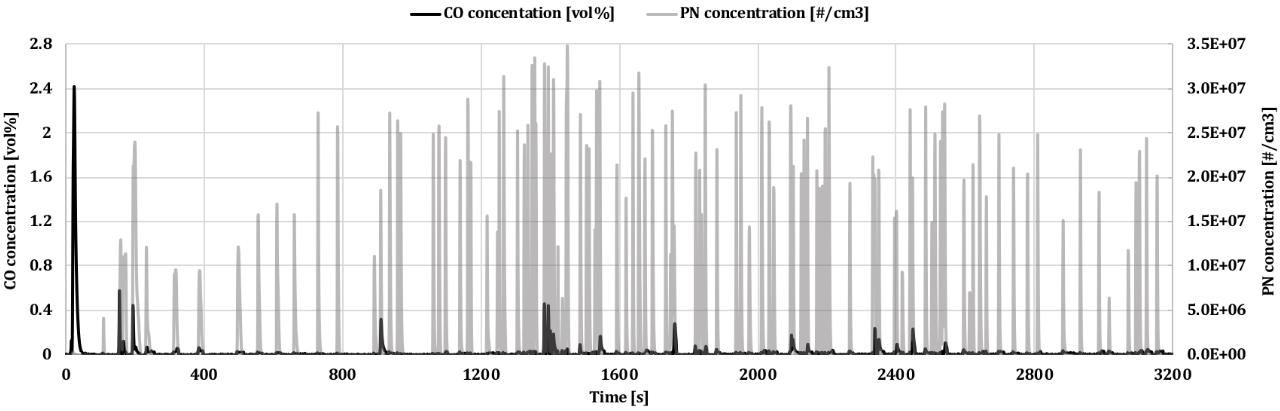

Fig.4 CO concentration vs. PN concentration of the PFI-HEV within the urban driving stage

In addition to fuel enrichment, the relatively low temperatures of the exhaust system when engine restarted can be another reason for the extra PN emissions from this PFI-hybrid vehicle. As shown in Fig.3, the exhaust temperatures measured at the tailpipe exit dropped some 20-70°C when engine restarted after a pause with the exhaust temperature being between 50°C and 125°C during the majority of the urban trip. Although exhaust temperature is less explicit than catalyst temperature at demonstrating catalyst efficiency, it is still a good metric showing how the temperature changed in the exhaust system for the nice agreement between the two temperatures has been shown in previous papers (Petkovic, Pesic, and Lukic 2011; Obodeh and Ogbor 2009). Generally, a substantial decrease in the temperature of the exhaust system jeopardized PN. It is plausible that the catalyst temperature of this PFI-hybrid had dropped below the light-off temperature within some engine-start events, causing the restricted conversion efficiency of the TWC. Untreated exhaust emissions were piped out in the initial few seconds after engine-start and contributed a lot to the extra PN emissions.

Unlike on ICE-only cars, the engine of this PFI-HEV worked in a generator-like strategy within the urban driving stage, where the engine typically ran only 10 to 20 seconds to charge the battery to a pre-determined battery SOC level and then switched off. Such a power management strategy guarantees very good fuel economy but may cause emission issues since it cools down the TWC quite frequently with additional air cooling outside.

This problem may not be unique for hybrid vehicles, it could happen on some modern models with idle stop-and-go (ISG) functions as well. Nevertheless, this problem for the vehicles with ISG systems will be less tricky compared to HEVs, since ISG systems only function at idle but the catalysts of HEVs receive extra air-cooling when the engine turns off while cruising, decelerating or traveling downhill. For HEVs, either decreasing the frequency of engine-stop or increasing the TWC temperature via external heating and/or thermal isolation may be helpful to mitigate this issue, but both measures will slightly increase fuel consumption. The “trade-off” relationship between fuel economy and particulate emissions must be carefully balanced.

Fig.5 illustrates the second-by-second vehicle speeds, engine speeds, exhaust temperatures, battery SOC levels, and throttle positions versus PN concentrations of the GDI-hybrid test vehicle within the urban driving stage. Similar to the PFI-hybrid case, a large number of PN spikes can be observed throughout the urban trip.

Since good correspondences among the PN spikes, engine-start events and decreases in the temperature of TWC are also found with this GDI-hybrid vehicle, it is reasonable to deduce that the formation of extra PN emissions is also induced by 1) enriched air-fuel mixture combusted within engine-starts, and 2) restricted TWC conversion efficiency due to decreased temperature of the exhaust system. Compared to the maximum PN readings of the PFI-HEV, PN emitted from this GDI-HEV was about 1/3 higher and reached 4.0E+7 #/cm^3. Though the PN concentration of this GDI-HEV in each single high-PN event was to various degrees higher than that of the PFI-HEV, the occurrence of high-PN events with this GDI-HEV was less frequent due to fewer engine-starts, underlying the comparably lower distance-based PN emission of this GDI-HEV within the urban driving stage. This comparison could also highlight the contribution of frequent engine-start to high real driving PN emissions.

The picture showing battery SOC level in Fig.5 is a good example of how the power management strategy decided the timings of engine-on and off and impacted the PN emissions of this GDI-HEV. In general, the control unit of the car endeavored to maintain the SOC level between 40% and 65% during the urban trip, the same as described previously in the discussion of the PFI-HEV. The timings to start or stop the engine show strong reliance on the vehicle speed, acceleration and current SOC level instead of depending upon emission control needs.

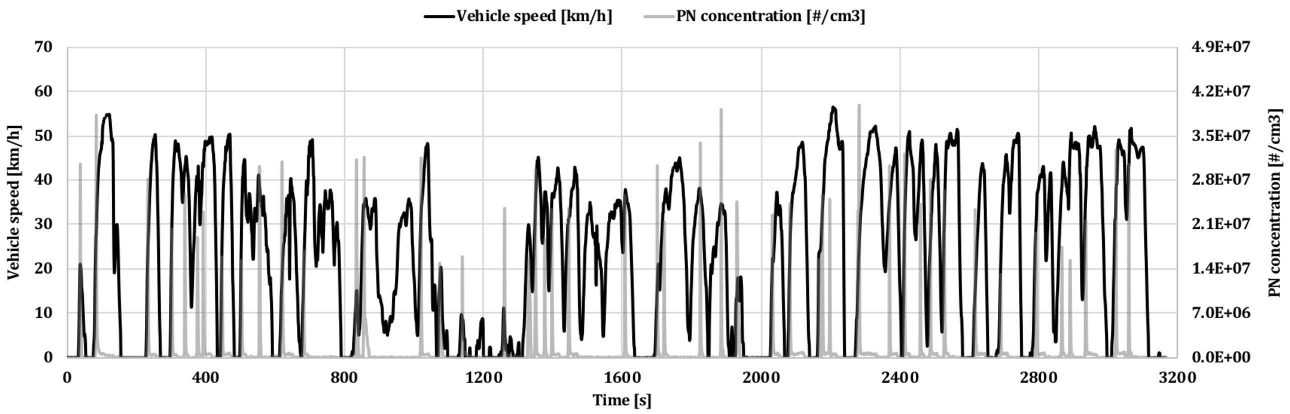

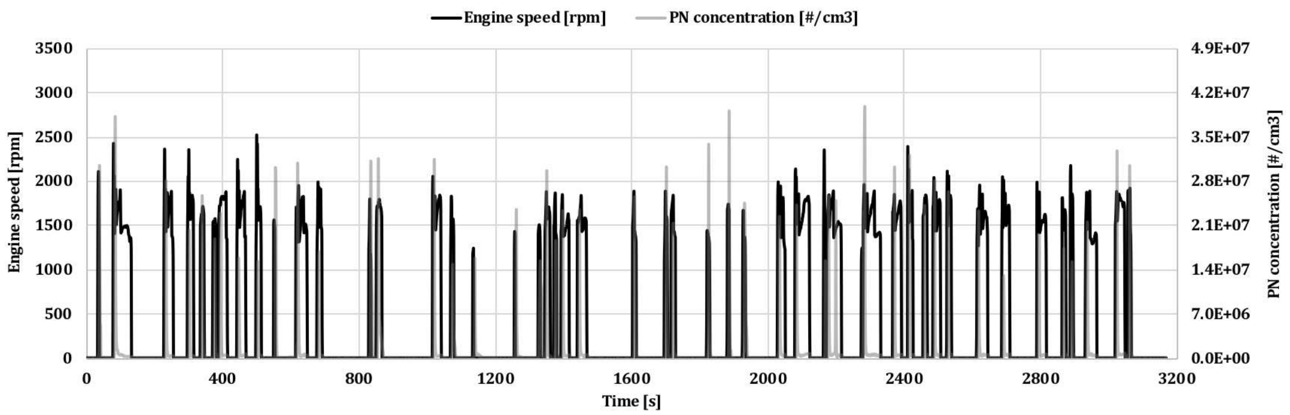

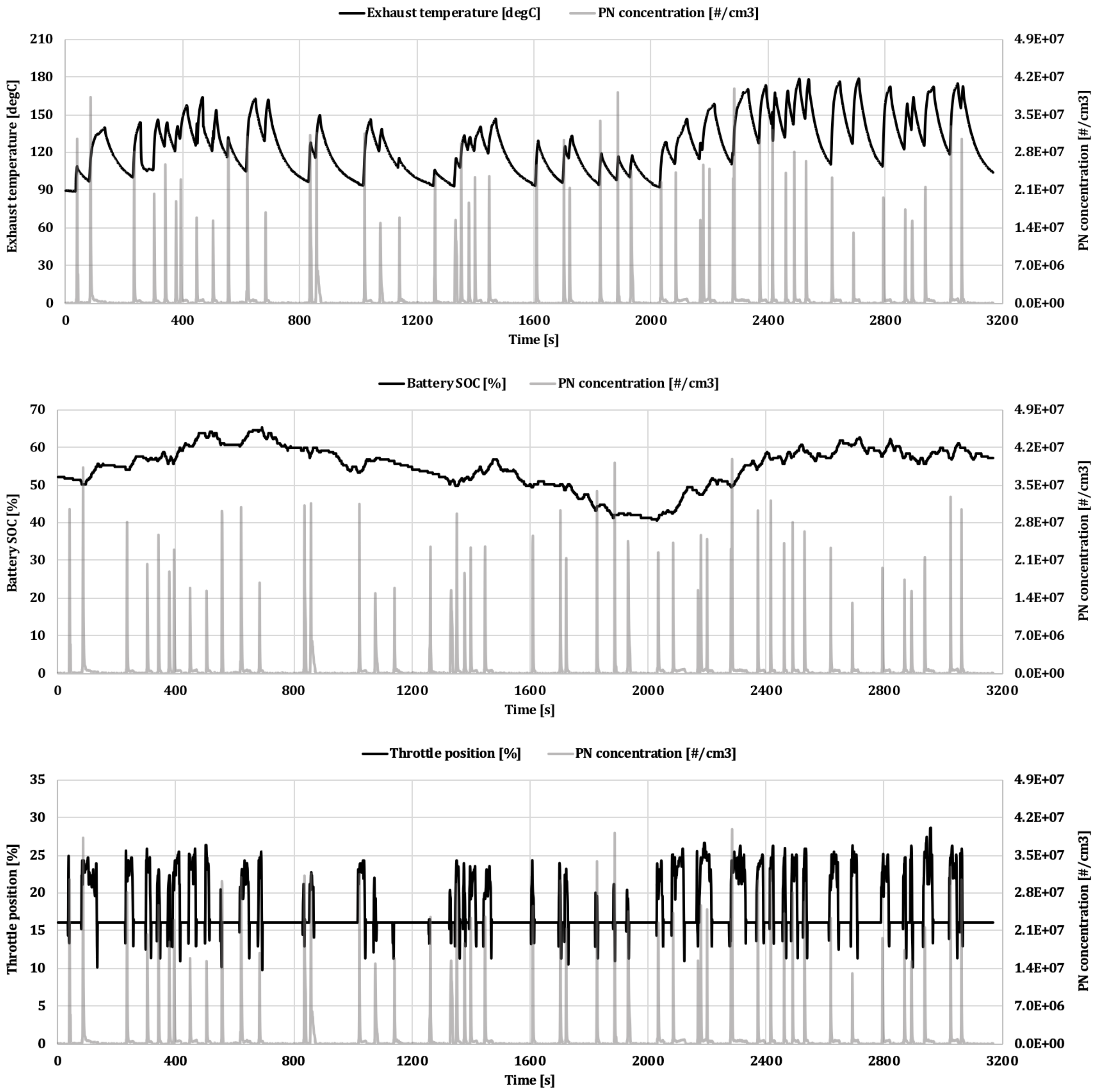

Fig.5 Vehicle speed, engine speed, exhaust temperature, battery SOC level, and throttle position versus PN concentration of the GDI-HEV within the urban driving stage

The higher PN emissions can be also attributed to the nature of GDI engines. Different from PFI engines, GDI engines inject fuel directly into the combustion chambers only a few crank angles before the top dead center, so there is very limited time to finish the air-fuel blending process before ignition. Stronger heterogeneity in GDI engines gives rise to heavier PM and PN emissions in comparison to PFI counterparts. Recent research also demonstrated that even a GDI engine starting with homogenous air-fuel mixtures could yield an excessive amount of solid PN emissions with non-measurable soot weight (Bock et al. 2018), let alone one with enriched air-fuel mixtures.

Hence, there is an argument against the integration of a GDI engine into a hybrid propulsion system. Although extra fuel economy benefit could be gained with GDI engines, their particulate emissions – not only PN but also PM – could be quite problematic. Again, for HEVs, the “trade-off” relationship between fuel economy and particulate emissions requires more considerations.

3.2 PN emissions in rural and highway driving

For conciseness, rural driving and highway driving are discussed together in this paper, mainly because in China, the driving behaviors on rural roads and highways share lots of similarities.

Fig.6 illustrates the vehicle speeds, engine speeds, exhaust temperatures, and intake mass flow rates versus PN concentrations of the PFI-hybrid test vehicle within rural and highway driving stages. It is easy to recognize that this vehicle implemented different power management strategies in rural and highway modes. The strategy for rural driving was more or less similar to the strategy in urban, where the engine was frequently switched on and off to maximize fuel saving, but vast PN emissions were produced. An exception was the duration from 3730s to 3950s, the engine kept running within this period so that the PN emissions were only 1.8E+3 to 4.2E+4 #/cm^3.

Compared to the urban and rural driving stages, the power management strategy during highway driving was more traditional and ICE-only-like. When this PFI-HEV was accelerated to 80km/h and faster, the engine only stopped as a consequence of a U-turn operation done by the man driver near ~4900s, which was undoubtedly not highway driving behavior. A plausible reason for this more traditional power management strategy used at high speeds is that it was no longer economic or possible to propel the car solely with the motor, then engine intervention is needed. The power consumed by a running vehicle is theoretically the sum of its aerodynamic drag, tire friction, acceleration, road-grade resistance and the inertia of rotating parts. Since it is proportional to the third power of vehicle speed, the aerodynamic drag is the dominant resistance and increases markedly when a vehicle cruises at high speeds. It can be estimated that the road load of this PFI-HEV had been roughly 40kW when it ran at a constant speed above 100km/h. Given that the rated power of the electric motors in hybrid systems is typically not high, the car would not be able to accelerate if the engine was still out of work. Another important reason for engine intervention during highway driving was that the engine had to keep charging the power battery since the energy consumption at high speeds was very fast. This behavior can be more clearly elaborated by the GDI-hybrid vehicle in Fig.7.

It can be seen in Fig.6 that the intervention of the engine benefited PN reduction due to the hotter engine and TWC. Within the highway driving stage, a few PN spikes can be only found at the end of the test where the engine became frequently stop-and-go again. In most of the highway driving, the concentrations of PN were 1.0E+3 to 5E+4#/cm^3, much lower than those seen within engine-start events. The fully warmed-up engine increased the temperature of its intake charge, promoting the homogeneity of the air-fuel mixture so reducing PN formation resulting from pool-fire and local fuel-rich combustion by a substantial scale (Kayes et al. 2000). In addition, an increase in the TWC temperature also promoted the conversion efficiency, helping remove a big part of the engine-out PN emissions.

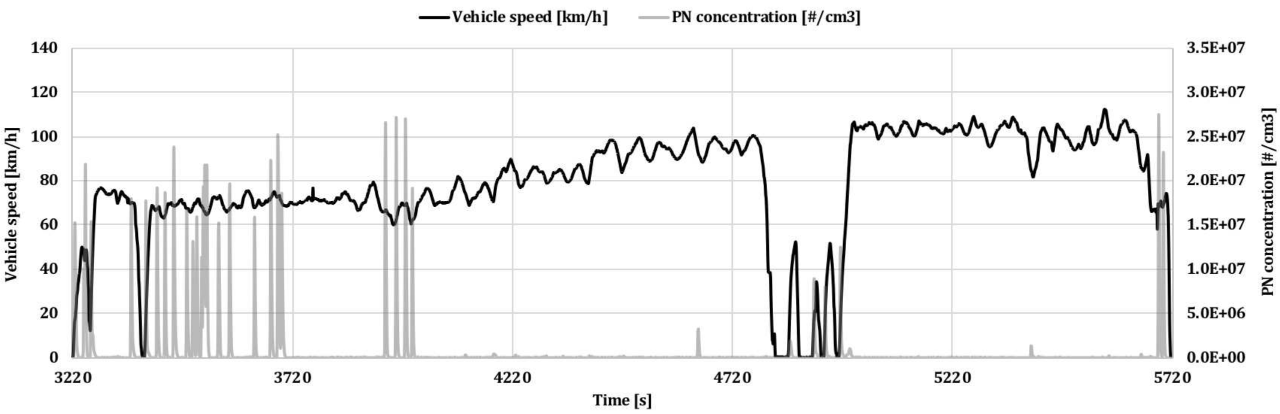

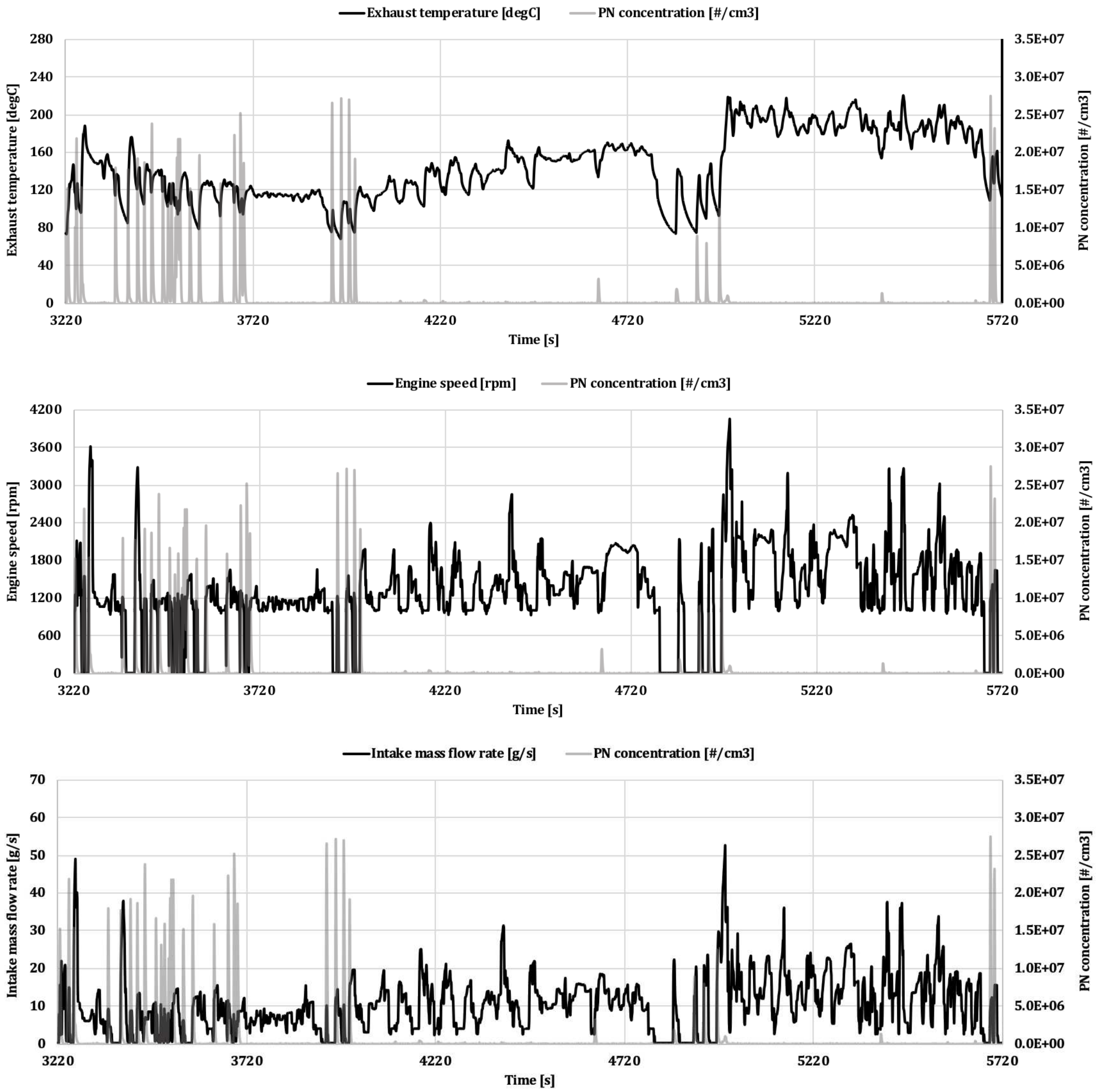

Fig.6 Vehicle speed, engine speed, exhaust temperature, and intake mass flow rate vs. PN concentration of the PFI-HEV within the rural and highway driving stages

It is also worth noting that the ranges and profiles of the engine speed and exhaust temperature from 3220s to ~3970s were generally comparable to those from ~3970s to 4720s, however, the PN emissions within these two time-windows were quite distinguished. With fewer engine-stops, the PN emissions within the latter window were much smaller. This contrast highlights the contribution of engine stop-and-go to extra PN emissions.

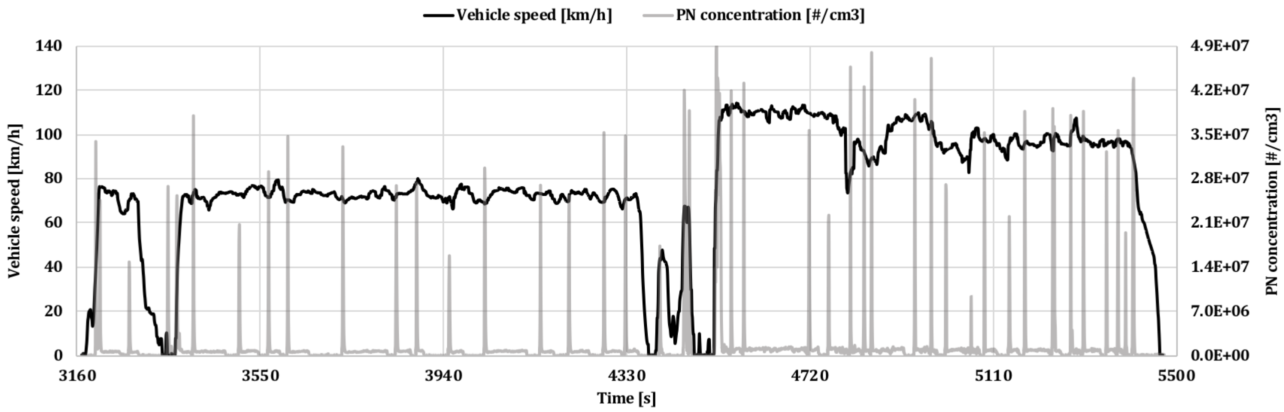
Vehicle speed [km/h]
PN concentration [#/cm3]
Vehicle speed [km/h]
PN concentration [#/cm3]
Time [s]
0 20 40 60 80 100 120 140
0.0E+00 7.0E+06 1.4E+07 2.1E+07 2.8E+07 3.5E+07 4.2E+07 4.9E+07
3160 3550 3940 4330 4720 5110 5500

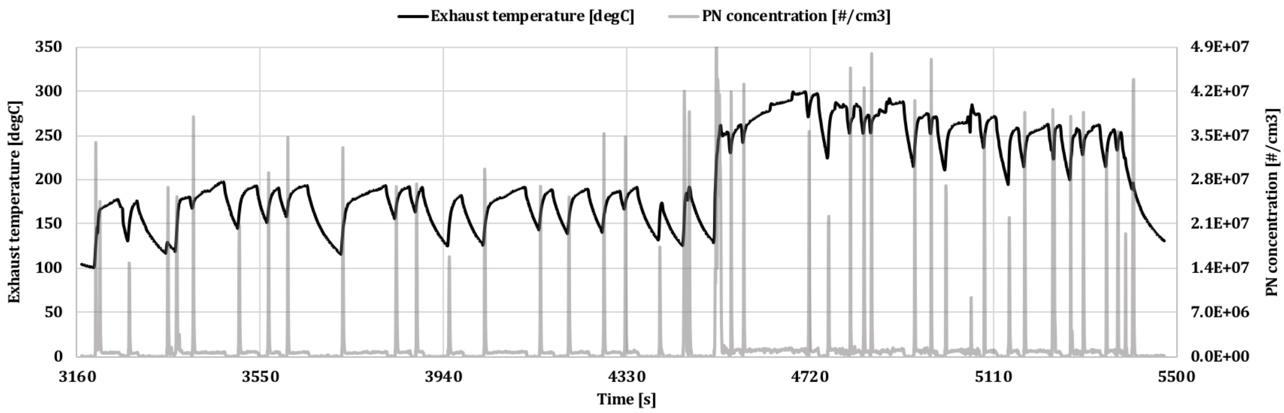
Exhaust temperature [degC]
PN concentration [#/cm3]
Exhaust temperature [degC]
PN concentration [#/cm3]
Time [s]
0 50 100 150 200 250 300 350
0.0E+00 7.0E+06 1.4E+07 2.1E+07 2.8E+07 3.5E+07 4.2E+07 4.9E+07
3160 3550 3940 4330 4720 5110 5500

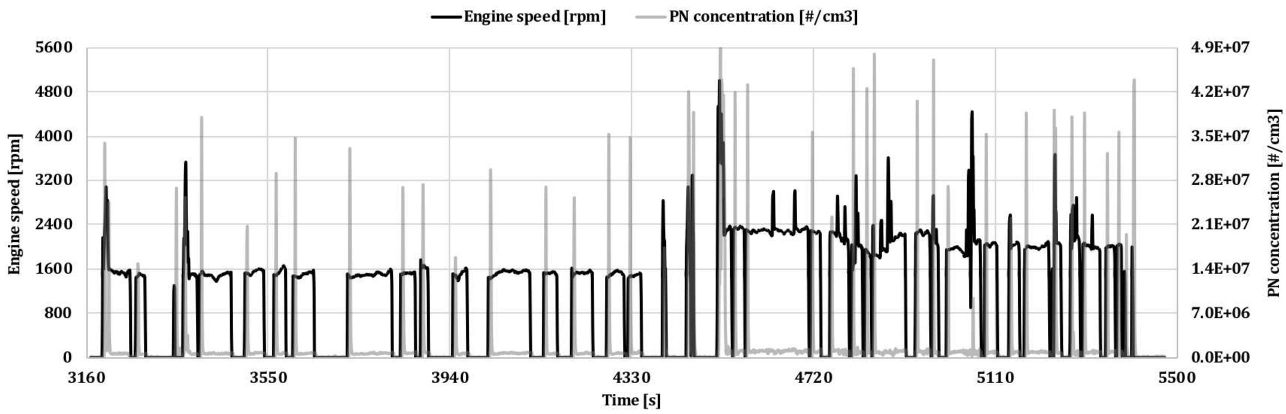
Engine speed [rpm]
PN concentration [#/cm3]
Engine speed [rpm]
PN concentration [#/cm3]
Time [s]
0 800 1600 2400 3200 4000 4800 5600
0.0E+00 7.0E+06 1.4E+07 2.1E+07 2.8E+07 3.5E+07 4.2E+07 4.9E+07
3160 3550 3940 4330 4720 5110 5500

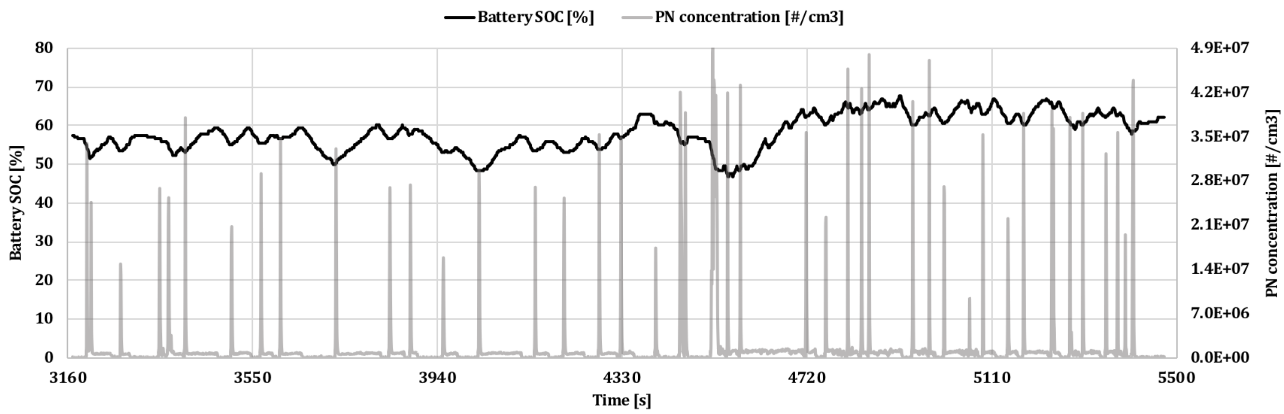
Battery SOC [%]
PN concentration [#/cm3]
Battery SOC [%]
PN concentration [#/cm3]
Time [s]
0 10 20 30 40 50 60 70 80
0.0E+00 7.0E+06 1.4E+07 2.1E+07 2.8E+07 3.5E+07 4.2E+07 4.9E+07
3160 3550 3940 4330 4720 5110 5500

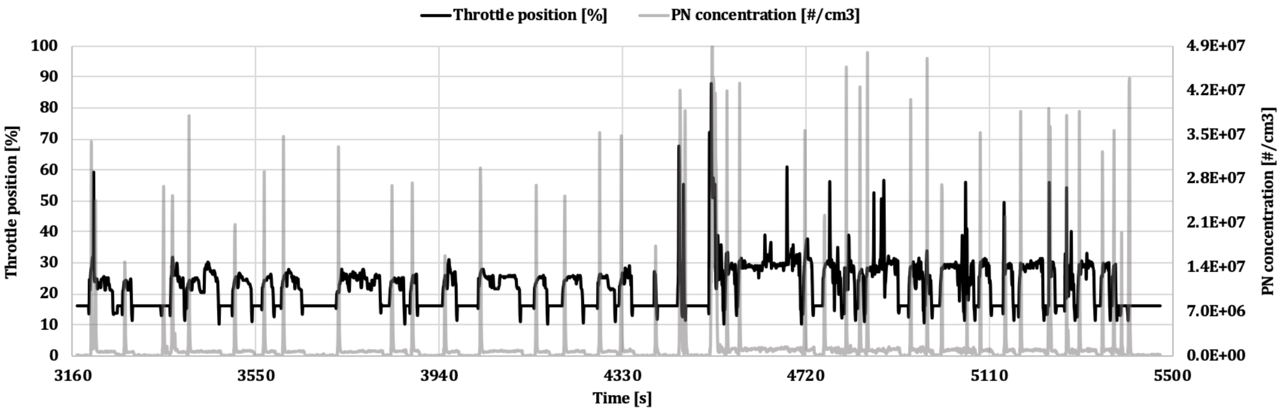

Fig.7 Vehicle speed, engine speed, exhaust temperature, battery SOC level, and throttle position versus PN concentration of the GDI-HEV within the rural and highway driving stages

Fig.7 displays the vehicle speeds, engine speeds, exhaust temperatures, battery SOC levels, and throttle positions versus real-time PN concentrations of the GDI-HEV. Unlike the PFI-HEV, within the rural and highway driving stages, this GDI-HEV used the same power management strategy as during urban driving. Within the rural driving period, the time between two engine pauses seems slightly lengthened, but several PN spikes corresponding to engine-starts can be still found in Fig.7. In the highway driving stage, the occurrence of high-PN events became dense again, because higher vehicle speed led to faster battery consumption and increased the frequency of engine-start for battery charging. It can be seen in the pictures illustrating engine speed and throttle position that the engine speed was raised from 1600r/min to 2400r/min and the throttle openness was also enlarged so as to realize faster charging under highway operating conditions.

The SOC profile depicted in Fig.7 well presents the power management strategy currently prevalent in market-available HEVs, which can be called "solely SOC-targeting strategy". The aim of this strategy is to achieve the best fuel economy, and the measure is to use the electric motor as much as possible with the engine running in generator-like, steady-state conditions, and the SOC level of the power battery is maintained within preset ranges which co-determine the engine operating conditions and PN emissions. Once the present SOC level goes below the preset threshold, the engine will be turned on to charge the battery and then shut off immediately after reaching the target value. It can be seen in Fig.7 that in this principle, the SOC level was well maintained between 45% and 70% during the rural and highway driving of the GDI-HEV tested.

Via the SOC level, energy consumption rate of the battery indirectly influences engine operating conditions and PN. Within the urban driving stage, as shown in Fig.5, the engine of the GDI-HEV only operated for a few seconds since the energy consumption at low speeds was small. Battery consumption became faster while the vehicle speeded up, hence it can be seen in Fig.7 that the engine ran for a much longer time at constant speeds after each start in the rural and highway modes, which helped reduce the frequency of engine-start and PN emissions.

Although this "solely SOC-targeting strategy" has been proven effective at delivering splendid fuel economies, it may unintendedly overlook the issue with extra PN emissions due to the absence of RDE requirements before. Since the new regulation will be soon implemented more widely, this drawback associated with over-frequent engine stop-and-goes seems quite problematic and calls more attention.

Fig.7 also offers a comparison between the PN emissions emitted within engine-start events and steady-state engine operations. It can be observed that the PN emissions were roughly 2E+5 to 1.2E+6#/cm^3 when the engine operated at 1600 and 2400r/min. By contrast, the engine-starts resulted in much greater PN emissions, which were one to two orders of magnitude larger and up to 4.9E+7#/cm^3. Such big differences could also explain why some HEVs can have much higher PN emissions than the ICE-only counterparts as compared in Fig.2.

3.3 Discussion on the emission factors

Since both the test vehicles are China-6 compliant, their real driving PN emissions can be compared to the China-6 and Euro-6 limits, which is currently regulated at 1.26E+12#/km (CF=2.1) and 9E+11#/km (CF=1.5) respectively. It can be seen in Table.2 that both the HEVs tested failed the Euro-6 limit by exceedances of 34% and 99.3%. The PN emissions from the GDI-HEV also exceeded the relatively tolerative China-6 limit by a factor of 35.7%. Though the PFI-HEV managed to meet the China-6 limit, it was approaching the limit. Also, it should not be ignored that 82% of the PN emissions from this PFI-HEV were emitted within the urban driving stage. Considering the much higher population density in urban areas, it is very disconcerting to see such emission characteristics, since the extra PN emissions could substantially increase the exposure risk and induce adverse impacts on public health.

To tackle this PN issue, the following changes of HEV design may serve as possible solutions but still, encounter several technical challenges.

1) Power management strategy: in addition to fuel economy, more considerations for exhaust emissions shall apply, engine intervention is expected to be lengthened but this undoubtedly, to various degrees, sacrifices fuel economy.

2) External heating and/or thermal isolation of TWC: it may be difficult to determine when to start engine and heater without a reliable access to predict the motivations of drivers, and adding heaters will result in fuel economy losses.

3) Gasoline particulate filter: GPF may be a solution but also requires good thermal management as a prerequisite, because long-time low-temperature operations may render the regeneration process impractical and cause blockage of the monolith.

Conclusions

In view of the limited knowledge about the real-world PN emission characteristics of HEVs, two China-6 compliant vehicles – a PFI-HEV and a GDI-HEV – were tested in this paper using a certification-level PEMS and strictly following the regulatory procedures for RDE testing. The results demonstrate that the PN emission factors for the PFI- and GDI-HEVs were 1.15E+12 and 1.71E+12#/km respectively, to various degrees exceeding those from the ICE-only counterparts and the upcoming regulatory RDE limits. More than 80% of the PN emissions from the PFI-HEV in the RDE trip were found in the urban driving stage, which may increase the exposure level of the public to ultrafine particles and pose health concerns. By analyzing the modal PN concentrations in contrast to the several parameters obtained from the OBD, one can conclude that enriched air-fuel mixtures and restricted TWC efficiencies associated with the more frequent stop-and-goes of the HEV engines are likely the underlying reasons for the extra PN emissions. To deal with the PN issue, amendments to the currently prevalent “SOC-oriented” power management strategy are required, despite challenges.

It is also understood that with only two test vehicles, it would be presumptive to conclude that the in-service HEVs are high PN emitters. However, the results of this paper highlight that some HEVs can encounter PN issues that might have been unintendedly overlooked in the past, and call on more attention to this problem.

Acknowledgements

This study received funding support from the National Natural Science Foundation of China (Grant No. 51806015), the National Postdoctoral Program for Innovative Talents of China (Grant No. BX201700032), the China Postdoctoral Science Foundation (Grant No. 2018M631354), and the Open Research Fund of the State Key Laboratory of Engine Combustion (Grant No. K2018-11).

Abbreviations

BEV: Battery Electrical Vehicle
CF: Conformity Factor
CPC: Condensed Particle Counter
EEPS: Engine Exhaust Particle Sizer
ELPI: Electrical Low Pressure Impactor
GDI: Gasoline Direct Injection
GPF: Gasoline Particulate Filter
GPS: Global Positioning System
HEV: Hybrid Electrical Vehicle
ICE: Internal Combustion Engine
ISG: Idle Stop-and-Go
NA: Naturally Aspirated
NG: Natural Gas
NTE: Not-to-exceed
OBD: On-board Diagnostic
PEMS: Portable Emission Measurement System
PFI: Port Fuel Injection
PM: Particulate Matter
PMP: Particulate Measurement Program
PN: Particulate Number
RDE: Real Driving Emission
RPA: Relative Positive Acceleration
SOC: State of Charge
TWC: Three-way Catalyst
$v.a_{pos-}$[95]: 95 percentile of the positive values of velocity times acceleration

References

Al-Samari, Ahmed. 2017. “Study of Emissions and Fuel Economy for Parallel Hybrid versus Conventional Vehicles on Real World and Standard Driving Cycles.” *Alexandria Engineering Journal* 56 (4). Faculty of Engineering, Alexandria University: 721–26. doi:10.1016/j.aej.2017.04.010.

Bock, Noah, Joonho Jeon, David Kittelson, and William F. Northrop. 2018. “Solid Particle Number and Mass Emissions from Lean and Stoichiometric Gasoline Direct Injection Engine Operation,” 1–10. doi:10.4271/2018-01-0359.

Bordelanne, Olivier, Micheline Montero, Frédérique Bravin, Anne Prieur-Vernat, Olga Oliveti-Selmi, Hélène Pierre, Marion Papadopoulo, and Thomas Muller. 2011. “Biomethane CNG Hybrid: A Reduction by More than 80% of the Greenhouse Gases Emissions Compared to Gasoline.” *Journal of Natural Gas Science and Engineering* 3 (5). Elsevier B.V: 617–24. doi:10.1016/j.jngse.2011.07.007.

Christenson, Martha, Aaron Loiselle, Deniz Karman, and Lisa a Graham. 2007. “The Effect of Driving Conditions and Ambient Temperature on Light Duty Gasoline-Electric Hybrid Vehicles (2): Fuel Consumption and Gaseous Pollutant Emission Rates,” no. 3: 776–90. doi:10.4271/2007-01-2137.

Graver, Brandon M, H Christopher Frey, and Hyung-Wook Choi. 2011. "In-Use Measurement of Activity, Energy Use, and Emissions of a Plug-in Hybrid Electric Vehicle." *Environmental Science & Technology* 45 (20): 9044–51. doi:10.1021/es201165d.

Hesterberg, Thomas W, Christopher M Long, William B Bunn, Charles A Lapin, Roger O Mcclellan, and Peter A Valberg. 2012. "Health Effects Research and Regulation of Diesel Exhaust : An Historical Overview Focused on Lung Cancer Risk" 24 (February): 1–45. doi:10.3109/08958378.2012.691913.

Kayes, D, S Hochgreb, M M Maricq, D H Podsiadlik, and R E Chase. 2000. "Particulate Matter Emission During Start-up and Transient Operation of a {Spark-Ignition} Engine (2): Effect of Speed, Load, and {Real-World} Driving Cycles." *{SAE} Technical Paper*, no. 724: 1–1083. doi:10.4271/2000-01-1083.

Kean, Andrew J., Robert A. Harley, David Littlejohn, and Gary R. Kendall. 2000. "On-Road Measurement of Ammonia and Other Motor Vehicle Exhaust Emissions." *Environmental Science and Technology* 34 (17): 3535–39. doi:10.1021/es991451q.

Kittelson, D. B., W. F. Watts, J. P. Johnson, J. J. Schauer, and D. R. Lawson. 2006. "On-Road and Laboratory Evaluation of Combustion Aerosols-Part 2:. Summary of Spark Ignition Engine Results." *Journal of Aerosol Science* 37 (8): 931–49. doi:10.1016/j.jaerosci.2005.08.008.

Kittelson, David B. 1998. "ENGINES AND NANOPARTICLES : A REVIEW" 29 (5): 575–88.

Liu, Jia, Yunshan Ge, Xin Wang, Lijun Hao, Jianwei Tan, Zihang Peng, Chuanzhen Zhang, Huiming Gong, and Ying Huang. 2017. "On-Board Measurement of Particle Numbers and Their Size Distribution from a Light-Duty Diesel Vehicle: Influences of VSP and Altitude." *Journal of Environmental Sciences (China)* 57. Elsevier B.V.: 238–48. doi:10.1016/j.jes.2016.11.023.

Mendoza-Villafuerte, Pablo, Ricardo Suarez-Bertoa, Barouch Giechaskiel, Francesco Riccobono, Claudia Bulgheroni, Covadonga Astorga, and Adolfo Perujo. 2017. "NOx, NH3, N2O and PN Real Driving Emissions from a Euro VI Heavy-Duty Vehicle. Impact of Regulatory on-Road Test Conditions on Emissions." *Science of the Total Environment* 609 (x). The Authors: 546–55. doi:10.1016/j.scitotenv.2017.07.168.

O'Driscoll, Rosalind, Marc E.J. Stettler, Nick Molden, Tim Oxley, and Helen M. ApSimon. 2018. "Real World CO2and NOxemissions from 149 Euro 5 and 6 Diesel, Gasoline and Hybrid Passenger Cars." *Science of the Total Environment* 621 (x). Elsevier B.V.: 282–90. doi:10.1016/j.scitotenv.2017.11.271.

Obodeh, O., and A. D. Ogbor. 2009. "Improving the Performance of Two-Stroke Motorcycle with Tuned Adjustable Exhaust Pipe." *Research Journal of Applied Sciences, Engineering and Technology* 1 (2): 59–65.

Petkovic, Snezana, Radivoje Pesic, and Jovanka Lukic. 2011. "Experimental Verification of Mathematical Model of the Heat Transfer in Exhaust System." *Thermal Science* 15 (4): 1035–48. doi:10.2298/TSCI110517102P.

Robinson, Mitchell, and Britt Holmén. 2011. "Onboard, Real-World Second-by-Second Particle Number Emissions from 2010 Hybrid and Comparable Conventional Vehicles." *Transportation Research Record: Journal of the Transportation Research Board* 2233: 63–71. doi:10.3141/2233-08.

Sioshansi, Ramteen, and Paul Denholm. 2009. "Emissions Impacts and Benefits of Plug-In Hybrid Electric Vehicles and Vehicle-to-Grid Services Emissions Impacts and Benefits of Plug-In Hybrid Electric Vehicles and Vehicle-to-Grid Services" 43 (4): 1199–1204. doi:10.1021/es802324j.

Soylu, Seref. 2015. "Development of PN Emission Factors for the Real World Urban Driving Conditions of a Hybrid City Bus." *Applied Energy* 138. Elsevier Ltd: 488–95. doi:10.1016/j.apenergy.2014.11.001.

Wang, Haohao, Yunshan Ge, Lijun Hao, Xiaoliu Xu, Jianwei Tan, Jiachen Li, Legang Wu, et al. 2018. "The Real Driving Emission Characteristics of Light-Duty Diesel Vehicle at Various Altitudes." *Atmospheric Environment* 191 (July). Elsevier: 126–31. doi:10.1016/j.atmosenv.2018.07.060.

Wang, Tianyang, David C. Quiros, Arvind Thiruvengadam, Saroj Pradhan, Shaohua Hu, Tao Huai, Eon S. Lee, and Yifang Zhu. 2017. "Total Particle Number Emissions from Modern Diesel, Natural Gas, and Hybrid Heavy-Duty Vehicles during On-Road Operation." *Environmental Science and Technology* 51 (12): 6990–98. doi:10.1021/acs.est.6b06464.

Wu, Xiaomeng, Shaojun Zhang, Ye Wu, Zhenhua Li, Wenwei Ke, Lixin Fu, and Jiming Hao. 2015. "On–Road Measurement of Gaseous Emissions and Fuel Consumption for Two Hybrid Electric Vehicles in Macao." *Atmospheric Pollution Research* 6 (5): 858–66. doi:10.5094/APR.2015.095.

Xu, Guangju, Mingdi Li, Yang Zhao, and Qingzhang Chen. 2017. "Study on Emission Characteristics of Hybrid Buses under Driving Cycles in a Typical Chinese City." *Advances in Mechanical Engineering* 9 (10): 168781401772823. doi:10.1177/1687814017728238.

Yin, H, Y Ge, X Wang, L Yu, Z Ji, and W Chen. 2013. "Idle Emission Characteristics of a Light-Duty Diesel van at Various Altitudes." *Atmospheric Environment*. doi:10.1016/j.atmosenv.2013.01.012.